

# The effect of the main processing parameters on the geometry of amorphous metal ribbons during planar flow casting (PFC)

H. FIEDLER, H. MÜHLBACH, G. STEPHANI

*Zentralinstitut für Festkörperphysik und Werkstofforschung der Akademie der Wissenschaften der DDR, DDR 8027 Dresden, Postfach, German Democratic Republic*

Experimental work on PFC performed with some amorphous alloys is reported. The subject of the investigation is the relationship between the main processing parameters and the resulting ribbon thickness. Calculations applying Bernoulli's equation reveal the relationship between the ribbon thickness and substrate velocity, ejection pressure, nozzle slot breadth and crucible wheel gap distance. Empirical data from numerous experiments are in good agreement with the calculations. Ribbons with smooth surfaces and precise cross-sections can be obtained by melt spinning with a small gap distance. The efficiency of a constrained melt puddle on the ribbon surface was exhibited by topographic measurements and high-speed motion pictures. Results of surface tension measurements have been used to explain the effect of the melt temperature on the ribbon thickness. Calculations and experimental data are a base for practical use of the PFC process in the production of ribbons with predetermined precise cross-section.

## 1. Introduction

The main processes for continuous casting of rapidly quenched amorphous alloy strips are chill block melt spinning (CBMS) and planar flow casting (PFC) [1]. In the CBMS process a free jet of liquid metal is ejected from a circular nozzle on the surface of a rapidly rotating roller. At a sufficient nozzle–roller gap distance the puddle formed at the point of impingement is free to spread laterally. The ribbon width is limited to about 4 mm. In order to produce wider ribbons the PFC technique with rectangular-shaped nozzles and small gap distances is used. Here the puddle is mechanically constrained between the nozzle lips and the wheel.

Numerous authors have studied the influence of the CBMS process variables on the dimensions of amorphous metal ribbons [2–7]. There are only a few reports dealing with results on ribbons produced by PFC [8–11]. This paper provides further information on ribbon formation by planar flow casting using nozzles with rectangular cross-section. The influence of the following process

variables on the ribbon geometry has been investigated: substrate velocity,  $v_s$ ; ejection pressure,  $p$ ; nozzle slot breadth,  $a_n$ ; nozzle-wheel gap,  $g$ ; injection angle,  $\alpha$ ; and temperature of the melt,  $T$ .

Liebermann and Graham [2] and Kavesh [4] have derived the effect of CBMS process parameters on the dimensions of melt-spun ribbons. To simplify the calculation the melt is assumed to be an ideal incompressible fluid. In a stationary state the liquid metal during ejection from the orifice follows Bernoulli's equation

$$v_j = \left( \frac{2p}{\rho} \right)^{1/2} \quad (1)$$

combined with the continuity equation

$$A_j v_j = A_r v_r \quad (2)$$

where  $A_j$  is the cross-sectional area of the jet,  $v_j$  is the velocity of the jet,  $A_r$  is the cross-sectional area of the ribbon,  $v_r$  is the velocity of the ribbon which is equal to the velocity of the rotating substrate. It has been further assumed that the

density,  $\rho$ , of the liquid melt is the same as that of the solid ribbon. Combination of Equations 1 and 2 leads to

$$A_r = \frac{A_j}{v_s} \left( \frac{2p}{\rho} \right)^{1/2} \quad (3)$$

In CBMS both the ribbon thickness,  $d$ , and the ribbon width,  $w$ , are influenced by changing the process parameters  $A_j$ ,  $v_s$  and  $p$ .

The present experiments carried out with the PFC technique reveal that the width of the ribbon is nearly equal to the length of the rectangular slot. Dividing Equation 3 by  $w$  gives the ribbon thickness

$$d = \frac{a_n}{v_s} \left( \frac{2p}{\rho} \right)^{1/2} \quad (4)$$

where  $a_n$  is the nozzle slot breadth.

A planar liquid metal jet having passed through the nozzle changes its shape in a characteristic way because of its surface tension [12, 13]. Therefore, the gap,  $g$ , between the nozzle and the wheel surface must be rather small. In this case the flow of the liquid metal is diminished by the distance between the nozzle and the rotating wheel. Additionally, the metal flow is influenced by superheating the melt, by its surface tension,  $\sigma$ , and also viscosity  $\eta$ . The effects of  $g$ ,  $T$ ,  $\sigma$  and  $\eta$  have been taken into consideration by inserting the proportionality factor  $K$  into Equation 4 leading to

$$d = K \frac{a_n}{v_s} \left( \frac{2p}{\rho} \right)^{1/2} \quad (5)$$

## 2. Experimental details

The equipment used and earlier described by Fiedler and Illgen [14], consisted of an  $\text{Al}_2\text{O}_3$ -ceramic crucible positioned in a vessel with a swivelling cover (Fig. 1). Melting was performed by r.f.-induction heating under vacuum or in many cases using a protective gas. A stopper system was used similar to ladle-pouring practice to prevent the melt from flowing out before superheating was accomplished. The temperature was controlled by an immersion thermocouple, and out-flow was aided by additional argon pressure. Orifices were made of heat resistant steel, ceramic or quartz, and rendered gas tight by a flange to the crucible. The copper wheel below the vessel (diameter 400 mm and width 65 mm) worked without water cooling. Another smaller device used on a laboratory scale was of a type from the well known

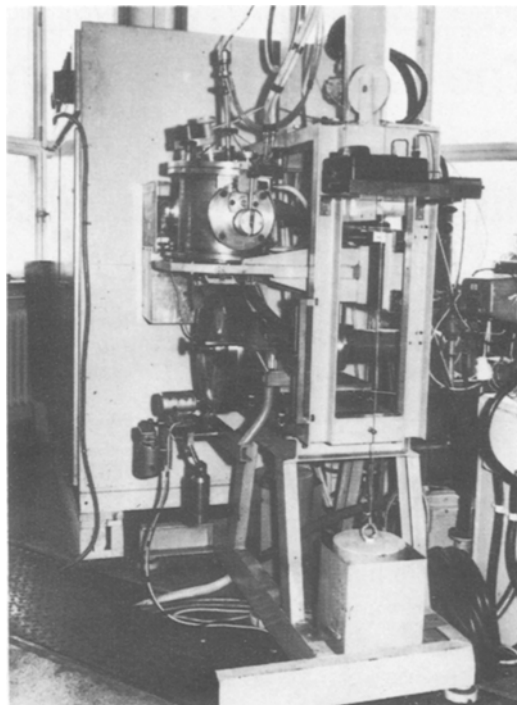


Figure 1 Melt-spinning apparatus with a 400 mm copper wheel suitable for 1 kg melting weight.

and frequently described system [2] involving a quartz tube, with a rectangular orifice, r.f.-induction heating, and a 180 mm copper disc. The alloys for our experimental procedures;  $\text{Fe}_{40}\text{Ni}_{40}\text{P}_{14}\text{B}_6$ ,  $\text{Fe}_{80}\text{B}_{20}$ ,  $\text{Fe}_{81}\text{B}_{13.5}\text{Si}_{3.5}\text{C}_2$ ,  $\text{Co}_{69}\text{Fe}_{4.5}\text{Cr}_2\text{Si}_{2.5}\text{B}_{22}$ ,  $\text{Fe}_{70}\text{Cr}_{10}\text{B}_{13}\text{C}_7$ , were premelted in a vacuum-induction furnace. Castings were carried out in air after remelting the master alloys in amounts of 20 to 1000 g. The velocity of the wheel was maintained between 15 and 35  $\text{m sec}^{-1}$  with both sets of apparatus. The examined range of distances between the nozzle and the wheel surface was 0.1 to 0.6 mm, the ejection pressures ranging from 8 to 60 kPa, and the impinging jet angle between perpendicular ( $90^\circ$ ) and  $70^\circ$ . Surface tension measurements were performed according to the method of maximum bubble pressure, and the surface tension was calculated using Schroedinger's equation [15]. The mean ribbon thickness was calculated from the weight, divided by the width, length and density. The ribbon width was kept between 10 and 15 mm.

## 3. Results and discussion

Fig. 2 shows experimental results of the thickness of the ribbons made by PFC in a  $\text{Fe}_{40}\text{Ni}_{40}\text{P}_{14}\text{B}_6$

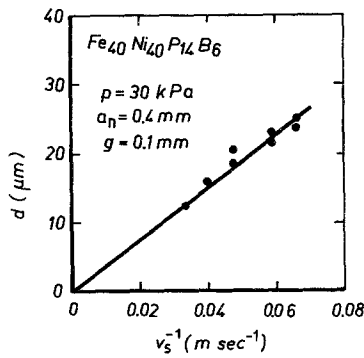


Figure 2 Ribbon thickness,  $d$ , as a function of the reciprocal of the wheel velocity,  $v_s^{-1}$ , at an ejection pressure of 30 kPa, slot breadth 0.4 mm, and gap distance 0.1 mm.

amorphous alloy as a function of the reciprocal of the substrate velocity. For other alloys, too, and the range of velocity examined, the ribbon thickness,  $d$ , depends on  $v_s^{-1}$  according to Equation 5. Takayama and Oi [9] have also derived a  $d \propto v_s^{-1}$  relationship for strip casting of amorphous alloys, but their experimental results seem to point to a somewhat different dependence. However, plotting their experimental data into a  $d \propto v_s^{-1}$  diagram, a straight line with little scatter can be obtained.

For  $Fe_{40}Ni_{40}P_{14}B_6$  and  $Fe_{81}B_{13.5}Si_{3.5}C_2$  alloys, Fig. 3 shows the dependence of the ribbon thickness,  $d$ , on the square root of the ejection pressure,  $p^{1/2}$ . Up to a pressure level of 60 kPa there is a linear correlation between  $d$  and  $p^{1/2}$  according to Equation 5. In contrast to these data, Huang [10] suggests a deviation of the  $d \propto p^{1/2}$  relationship when the ejection pressure exceeds 20 kPa, i.e. the thickness cannot be further increased with rising pressure at a given slot breadth and gap distance. It appears that Huang's

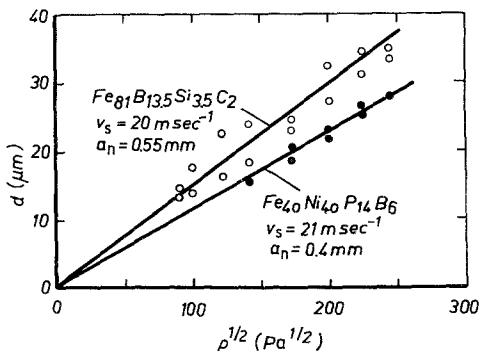


Figure 3 Ribbon thickness,  $d$ , as a function of the square root of ejection pressure,  $p^{1/2}$ , for  $Fe_{40}Ni_{40}P_{14}B_6$  and  $Fe_{81}B_{13.5}Si_{3.5}C_2$  amorphous alloys at a nozzle-wheel gap distance of 0.1 mm.

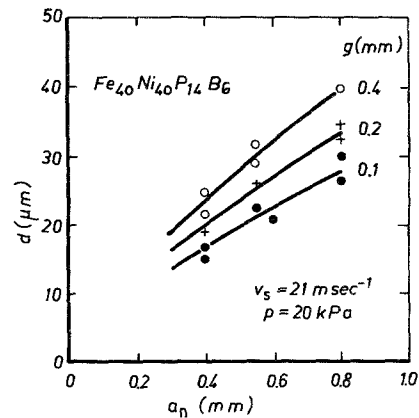


Figure 4 Ribbon thickness,  $d$ , as a function of the orifice slot breadth,  $a_n$ , for a given substrate velocity and ejection pressure at three nozzle-wheel gap distances,  $g$ . The empirical relationships correspond to  $d \propto a_n^{0.75}$ .

experimental procedure is characterized by a rather short slot length, and also a small slot length to width ratio, compared with our results. For those conditions the crucible-wheel gap adopted was large, so the increase in metal flow with increasing pressure supposedly resulted in an increase of ribbon width.

Ribbon thickness,  $d$ , is plotted against the slot breadth,  $a_n$ , for three nozzle wheel gap distances,  $g$ , in Fig. 4. The experimental data fit lines given by  $d \propto a_n^{0.75}$ . Fig. 5 shows the effect of the nozzle-wheel gap,  $g$ , on the ribbon thickness,  $d$ , which can be described by the proportionality  $d \propto g^{0.25}$ . Reconfirmation of this relation was obtained by experiments carried out at higher substrate velocities. Combining the results of Figs. 4

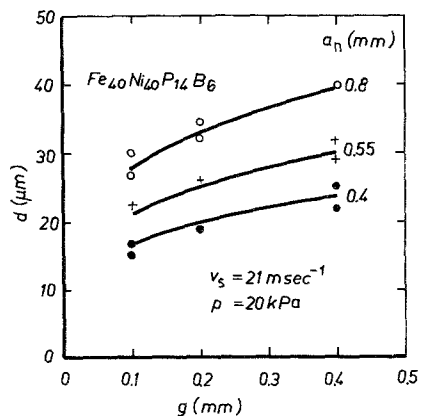


Figure 5 The effect of the nozzle-wheel gap distance,  $g$ , on the ribbon thickness,  $d$ , at three nozzle slot breadths,  $a_n$ . The plotted curves correspond to  $d \propto g^{0.25}$ .

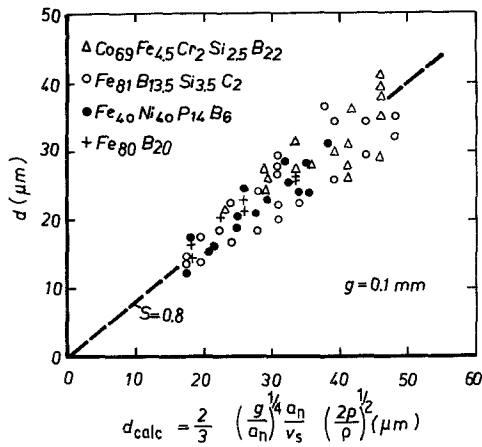


Figure 6 Variation of ribbon thickness,  $d$ , with calculated data from Equation 8 for some amorphous alloys at a nozzle-wheel gap distance of 0.1 mm. The slope of the curve is  $S = 0.8$ .

and 5, the ribbon thickness,  $d$ , is given by

$$d \propto g^{0.25} a_n^{0.75} = \left(\frac{g}{a_n}\right)^{0.25} a_n \quad (6)$$

When the gap,  $g$ , becomes equal to the slot breadth,  $a_n$ , the limiting effect of the gap on the metal flow ceases, and the ribbon thickness will be mainly controlled by the slot breadth,  $a_n$ , i.e.  $d \propto a_n$ .

Additionally it must be considered that the jet velocity,  $v_j$ , according to Equation 2, holds for frictionless flow only. When friction loss is taken into account the mean velocity of the liquid flow  $\bar{v}_j$  through a rectangular-shaped nozzle will be  $2/3$  of the velocity without friction,  $v_j$  [16], i.e.

$$\bar{v}_j = \frac{2}{3} v_j$$

The coefficient  $K$  of Equation 5 then becomes

$$K = \begin{cases} \frac{2}{3} \left(\frac{g}{a_n}\right)^{1/4} & \text{when } g < a_n \\ \frac{2}{3} & \text{when } g \geq a_n \end{cases} \quad (7)$$

Combination of Equations 5 and 7 gives an expression for the thickness of ribbons made by PFC

$$d = \frac{2}{3} \left(\frac{g}{a_n}\right)^{1/4} \frac{a_n}{v_s} \left(\frac{2p}{\rho}\right)^{1/2} \quad (8)$$

The experimental data for different amorphous alloys in Fig. 6 at a gap distance of 0.1 mm indicate a reasonably good agreement with Equation 8

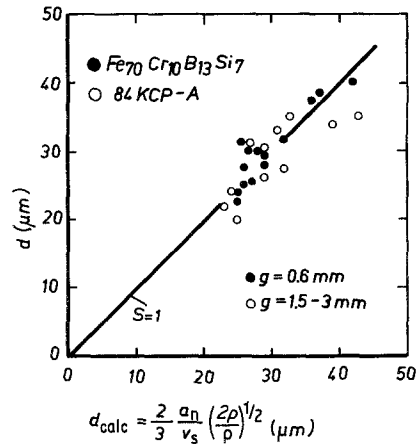


Figure 7 Ribbon thickness as a function of the processing parameters slot breadth,  $a_n$ , substrate velocity,  $v_s$ , and ejection pressure,  $p$ , for 84 KCP-A Co-rich amorphous alloy, and corrosion resistant alloy  $\text{Fe}_{70}\text{Cr}_{10}\text{B}_{13}\text{Si}_7$ . The slope of the curve is  $S = 1.0$ .

by this small scatter band, though the slope of the curve does not become 1.0. When the uncertainties in the exponents derived from Figs. 4 and 5,  $g^{0.25 \pm 0.03}$  and  $a_n^{0.75 \pm 0.05}$ , respectively, are inserted in Equation 6, the slope of Fig. 6 is changed by a factor of 0.82 for  $a_n = 0.55$  mm. Thus the exponents obtained experimentally are exact enough and convenient for practical use. The dependence of  $g$  and  $a_n$  derived from Equation 6 can be confirmed experimentally by the results of Huang [10]. In his paper,  $d$  is plotted as a function of the ratio  $a_n/g$  (Fig. 2 in [10]). By replotting his results according to Equation 6 a straight line through the origin is obtained. The maximum limit of the coefficient  $K = 2/3$  is attained by PFC at great distances between the nozzle and the moving substrate. This effect is indicated by data from Fig. 7 when the gap distance was kept almost at 0.5 mm. The empirical relationships between the ribbon thickness and the most essential processing parameters are given by the coefficient  $K = 0.66$  for two different amorphous alloys. Confirming experimental work was carried out at two laboratories under similar conditions [17] by different laboratory assistants.

Further experiments were carried out to examine the effect of the liquid jet angle impinging on the rotating substrate. The crucible-orifice unit was inclined from  $\alpha = 90^\circ$  (a jet perpendicular to the wheel surface) to  $\alpha = 70^\circ$ . In each case the nozzle outlet was very carefully fitted to the wheel surface by grinding, so that the gap distance

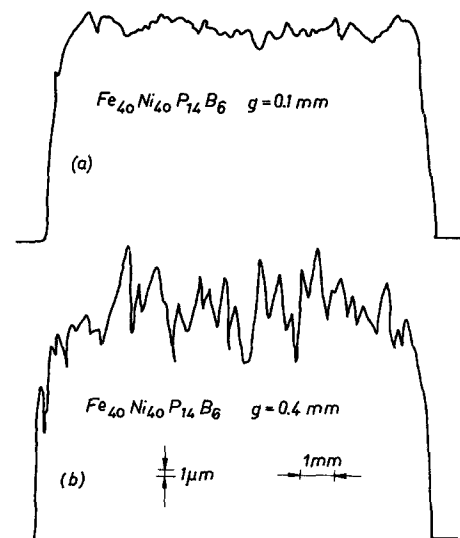


Figure 8 Microprofiles across the free sides of  $Fe_{40}Ni_{40}P_{14}B_6$  ribbons at crucible-wheel gap distances,  $g = 0.1$  mm (a) and  $g = 0.4$  mm (b).

was maintained. There was no effect on the ribbon thickness, nor the ribbon surface topography, within the range examined. From this it follows that the applied gap distance is the main controlling parameter of the ribbon thickness and not the angle of the impinging jet, if all the other processing parameters are kept unchanged. Working with the CBMS technique, other authors [6, 7] found that the influence of the angle on the ribbon thickness is rather distinct.

The gap distance between the nozzle and the roller surface has a remarkable effect on the ribbon surface finish.

When cast at small gap distances the melt puddle is constrained between the wheel surface and the nozzle, thus to a certain degree suppressing oscillations of the whole system which are transmitted to the solidifying ribbon and cause a rough surface at both sides. Surface topographies of orifice-sided ribbons (Fig. 8) show the effect of a 0.1 mm gap distance compared to a 0.4 mm indicated by the roughness profiles. As can be seen from the Fig. 8, a smaller gap distance results in a better quality ribbon.

Photographs of the melt puddles taken from high-speed motion pictures correspond to these experimental results. A puddle which is constrained by a small gap distance, exhibits smooth surfaces generally, and a perturbed puddle will result in a rough ribbon surface as seen in Fig. 8. It should be emphasized that all experiments

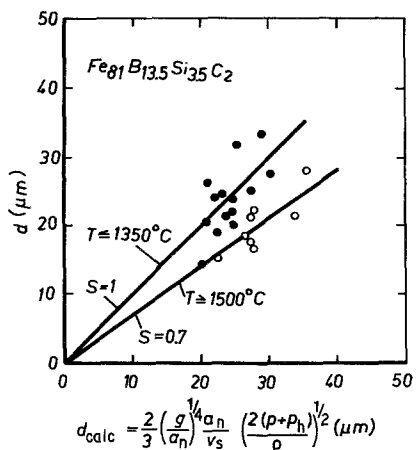


Figure 9 Ribbon thickness,  $d$ , as a function of the calculated ribbon thickness,  $d_{calc}$ , for ribbons cast at  $T \leq 1350^\circ C$  and  $T \geq 1500^\circ C$ . The slopes of the curves are  $S = 1$  and  $S = 0.7$ , respectively.

carried out used a special air-dissipating device which was positioned not more than 5 mm in front of the orifice, additionally preventing puddle perturbation.

Another metallurgically important parameter affecting the ribbon thickness is the melting temperature. It was suggested, that the scatter of the experimental points in Fig. 6 was partly due to deviations of the melt temperature. To check this parameter the equipment shown in Fig. 1 was particularly used, because temperature measurement could be performed more precisely. In this case the ferrostatic pressure,  $p_h$ , as a result of a larger melting weight in the crucible had to be considered, putting  $p + p_h$  into Equation 8.

The effect of the melt temperature on the ribbon thickness is shown in Fig. 9 for  $Fe_{81}B_{13.5}Si_{3.5}C_2$ . The experimental results were plotted for strips cast at temperatures up to  $1350^\circ C$  and above  $1500^\circ C$ . The lines were drawn through the origin according to Equation 8 and show the least squares best fit. The data agree quite well with the linear relationship expected from Equation 8 although there is some scatter in the data. Surprisingly, a higher melting temperature,  $T$ , causes a decrease in the ribbon thickness, although it was expected that the mass flow through the nozzle would be increased because of the lower viscosity. One explanation of this behaviour could be given by the surface tension. Therefore, the surface tensions of some amorphous alloys were measured under rising temperature conditions. The resulting data in Fig. 10 show remarkable differences in the

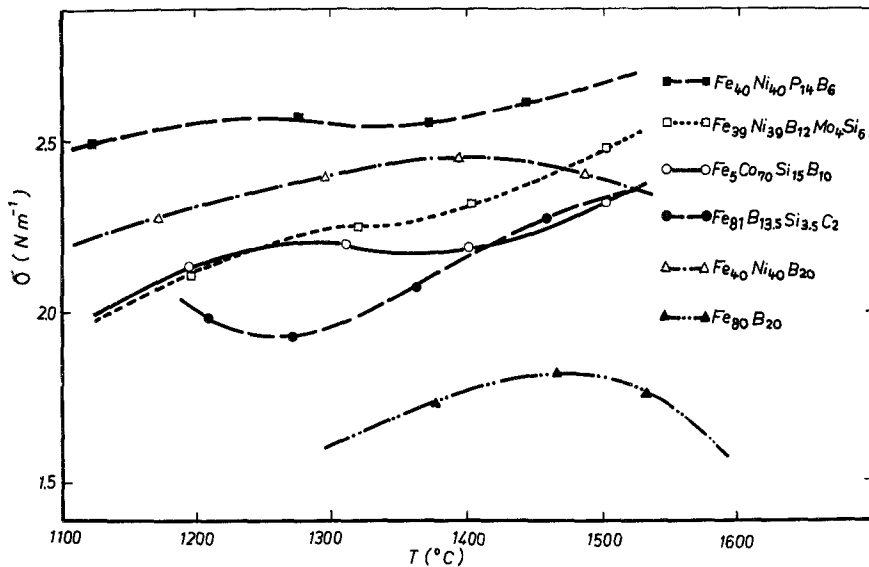


Figure 10 Relationship between the surface tension,  $\sigma$ , and the melt temperature,  $T$ , for some alloys.

surface tension–temperature dependence of the alloys. In the case of  $\text{Fe}_{81}\text{B}_{13.5}\text{Si}_{3.5}\text{C}_2$ , the surface tension increases between 1250 and 1500°C almost monotonically from  $1.85 \text{ N m}^{-1}$  to  $2.25 \text{ N m}^{-1}$  so that for this alloy the lower slope of the 1500°C line in Fig. 9 can be expected. On the other hand, Fig. 6 shows that the experimental points of the ribbon thickness lie in the same scatter band for different alloys although their surface tensions are quite different. Thus the temperature dependence of the surface tension is not sufficient to explain the effect of the melting temperature on the ribbon thickness. Another suggestion for explaining the dependence of the ribbon thickness on the melting temperature according to Fig. 9 will be the increasing mass transport of a liquid with higher viscosity (at a lower temperature) supported by the moving substrate, and the small gap distance applied.

#### 4. Conclusions

Operating conditions for 10 to 15 mm wide ribbons of some amorphous alloys have been explored using PFC. The ribbon thickness is controlled essentially by the ejection pressure,  $p$ , the wheel velocity,  $v_s$ , the slot breadth of the orifice,  $a_n$ , and the nozzle–wheel gap distance,  $g$ , according to the relationship

$$d = K \frac{a_n}{v_s} \left( \frac{2p}{\rho} \right)^{1/2}$$

with the coefficient  $K$  involving a combination of the nozzle–wheel gap distance, the nozzle slot breadth, and the influence of the melt superheating temperature. The ribbon surface roughness is strongly affected by the melt puddle which has to be free from periodically occurring jet turbulences or mechanical vibrations. It was proved, that spinning with a constraint puddle was most advantageous, i.e. applying a rather small and exactly adjusted gap distance between the nozzle and the wheel surface. It was found that gaps of 0.1 to 0.15 mm resulted in excellent nozzle-sided ribbon surfaces.

A suggested contradiction of the relationship between the ribbon thickness and the temperature of the melt for one Fe-base amorphous alloy could be explained by the specific behaviour of the surface tension with rising temperature for that particular alloy. However, the coefficient  $K$  in Equation 8 also implicates the viscosity.

#### Acknowledgements

The authors are grateful to Dr-Ing Kraus from the Bergakademie Freiberg for his assistance in surface tension measurements and for making special laboratory devices available for our experiments. We also thank Mr Reiche and Mr Hoehne for their complementary work in experimental preparation.

#### References

1. J. H. VINCENT, J. G. HERBERTSON and H. A. DAVIS, Proceedings of the 4th International Con-

- ference on Rapidly Quenched Metals, Sendai 1981, Vol. I (The Japanese Institute of Metals, Sendai, 1982) p. 77.
2. H. H. LIEBERMANN and C. D. GRAHAM Jr, *IEEE Trans. Magn.* MAG-12 (1976) 921.
  3. H. H. LIEBERMANN, *Mater. Sci. Eng.* 43 (1980) 203.
  4. S. KAVESH, "Metallic Glasses" (ASM, Metals Park, Ohio, 1978) p. 275.
  5. H. A. DAVIES, in "Rapidly Quenched Metals III", Vol. I (The Metals Society, London, 1978) p. 1.
  6. H. H. HILLMANN and H. R. HILZINGER, *ibid.* p. 22.
  7. D. PAVUNA, *J. Mater. Sci.* 16 (1981) 2419.
  8. M. C. NARASIMHAN, US Patent 4 142 571 (1979).
  9. S. TAKAYAMA and T. OI, *J. Appl. Phys.* 50 (1979) 1595, 4962.
  10. S. C. HUANG, General Electric Report No. 81 CRD 152 (1981).
  11. S. C. HUANG and H. C. FIEDLER, *Met. Trans. A* 12A (1981) 1107.
  12. W. JASCHINSKI, W. WOLF, U. KÖNIG and J. HARTWIG, *Techn. Mitt. Krupp, Forsch. Ber.* 39 (1981) 1.
  13. H. E. CLINE and T. R. ANTHONY, General Electric Report No. 78 CRD 066 (1978).
  14. H. FIEDLER and L. ILLGEN, Proceedings, 14 Metalltagung in der DDR, Akademie der Wissenschaften der DDR (Zentralinstitut für Festkörperphysik und Werkstofforschung, Dresden, 1981) p. 72.
  15. R. SCHROEDINGER, *Ann. Physik* 46 (1915) 413.
  16. W. ALBRING, "Angewandte Strömungslehre" (Verlag Theodor Steinkopff, Dresden, 1966).
  17. V. P. OVČAROV, unpublished results, Moscow (1981).

*Received 5 July*

*and accepted 14 December 1983*